Performance and Structure of Pt–Rh Three-Way Catalysts: Mechanism for Pt/Rh Synergism

Z. Hu,*,1 F. M. Allen,* C. Z. Wan,* R. M. Heck,* J. J. Steger,* R. E. Lakis,† and C. E. Lyman†

Engelhard Corporation, 101 Wood Avenue, Iselin, New Jersey 08830; and †Materials Science and Engineering Department, Lehigh University, Bethlehem, Pennsylvania 18015

The catalyst performance and structure of Pt and Rh catalyst systems are studied for fresh catalysts and samples aged to mimic in-use catalyst performance. It was observed that both fresh Pt and Rh catalysts are highly active for three-way conversions of HC/CO/NO. However, after exposure to exhaust at elevated temperature, Pt and Rh catalysts deteriorated severely, and only the Pt–Rh catalyst remains highly active for the three-way conversions. In order to understand this observed synergism between Pt and Rh in the Pt–Rh catalyst, AEM, XPS, and XRD were used to characterize catalyst structural change and establish a correlation between catalyst performance and structure. Pt catalysts deactivate at high temperature under reducing conditions and more severely under oxidizing conditions. Rh catalysts deactivate under oxidizing conditions by forming Rh–aluminate species. The regeneration of these Rh–aluminate species to highly active Rh metal particles under reducing conditions take place at elevated temperature, e.g., 1173 K, which is significantly higher than normal operating temperature (673 K). For the Pt–Rh catalyst, Pt and Rh go through deactivation cycles the same as that for the individual Pt and Rh catalysts in the simulated aging process. However, Rh in the aged Pt–Rh catalyst can regenerate in exhaust at temperatures as low as 560 K, which is significantly lower than the normal operating temperature. This is attributed to H_2/CO spillover on Pt particles contained in the Pt–Rh catalyst which facilitate the regeneration of the inert Rh–aluminate species to active Rh metal particles.   © 1998 Academic Press

INTRODUCTION

Pt–Rh three-way catalysts (TWCs) have been widely used to lower HC/CO/NO$_x$ emission from automobiles. Extensive research activities on the Pt–Rh TWC system have been reported and summarized in review articles (1, 2). Platinum is used as the catalyst for HC and CO oxidation. Rhodium is recognized as the catalyst to promote the reduction of NO to N_2 (3–5). As an oxidation catalyst for CO, the specific activity of Rh also compares favorably with Pt catalysts (6). Several articles report deactivation of Rh catalysts under oxidizing conditions (7, 8), which may be related to

the interaction of rhodium oxide with alumina support and the diffusion of rhodium into the bulk of alumina during calcination at 873 K or above (9, 10).

Three-way catalysts need to withstand high-temperature operation. It has been observed that exposure of catalysts to oxidizing conditions at high temperatures results in activity decrease, particularly for NO reduction and CO oxidation (4, 11, 12), which are generally attributed to Rh deactivation through transformation to the hard-to-reduce Rh–Al–oxide species (Rh–aluminate). The exposure of oxidized catalysts to reducing conditions restores some activity. Pt catalysts deteriorate after high-temperature exposure, which is attributed to Pt sintering and loss of active metal area.

Summarizing the literature, it is generally recognized that Rh is the primary active component in all three-way catalysts for NO$_x$ reduction. Rhodium also makes a significant contribution to CO oxidation. While Pt also catalyzes simultaneous HC/CO/NO conversions under typical three-way exhaust conditions, it is not as effective as rhodium particularly for NO reduction (1, 2). However, it is impossible to ascribe entirely independent functions to the two noble metals.

Studies of Pt–Rh interaction were reported in the literature (13, 14). We reported that a Pt/Rh synergism was operative in Pt–Rh three-way automotive catalysts (15). This study correlates catalyst activity with structure and proposes a new mechanism based on observed Pt–Rh synergism that Rh particles are the main active sites for three-way conversion and the Pt keeps the Rh in active Rh metal particles by regenerating nonactive Rh–aluminate species.

EXPERIMENTAL

Catalyst preparation. Gamma alumina powders of BET surface area 150 m²/g were used as catalyst support, and 62 cell/cm² ceramic monolith was used as the substrate. Pt/Al$_2$O$_3$ catalyst powders were prepared by impregnating amine-solubilized platinum hydroxide solution into the alumina powders according to incipient wetness procedure

---

[1] To whom correspondence should be addressed.

TABLE 1

Catalyst Compositions of Pt and Rh Catalysts

Catalyst	Pt + Rh loading (g/liter)	Washcoat loading (g/liter)
Pt/alumina	1.18 g Pt	61 g 1.9 wt% Pt/Al_2O_3 + 61 g Al_2O_3
Rh/alumina	0.24 g Rh	30.5 g 0.78 wt% Rh/Al_2O_3 + 91.5 g Al_2O_3
Pt–Rh/alumina	1.18 g Pt + 0.24 g Rh	61 g 1.9 wt% Pt/Al_2O_3 + 30.5 g 0.78 wt% Rh/Al_2O_3 + 30.5 g Al_2O_3

and then dried at 373 K for 12 h and calcined at 773 K for 2 h. Rh/Al_2O_3 catalyst powders were prepared using rhodium nitrate solution following the same procedure. Mixtures of Pt and Rh catalyst powders were then ball milled to reduce particle size to 90% less than 10 μm to form an aqueous slurry. The obtained slurry was then applied onto a ceramic honeycomb substrate. Excess slurry was blown off using forced air flow to obtain the desired catalyst compositions and then dried at 373 K for 12 h and calcined at 773 K for 2 h. Composition of Pt, Rh, and Pt–Rh monolithic catalysts are summarized in Table 1. For instance, the Pt–Rh/alumina catalyst contains 61 g 1.9 wt% Pt/Al_2O_3, 30.5 g Al_2O_3, and 30.5 g 0.78 wt% Rh/Al_2O_3, which is equivalent to a total Pt loading of 1.18 g, and Rh of 0.24 g, in 1 liter honeycomb substrate volume.

Catalyst evaluation. A laboratory honeycomb reactor was used to evaluate catalyst activity in a simulated auto exhaust gas stream using catalyst cores (3.8 cm in diameter and 7.6 cm in length). There was a main feed stream to the reactor, containing about 0.3% CO, 0.1% H_2, 0.35% O_2, 16.3% CO_2, 10% H_2O, 1600 ppm NO, 280 ppm C_3H_8, 280 ppm C_3H_6, and 40 ppm SO_2 with the balance nitrogen. A side stream of air and a second side stream of CO and hydrogen were injected alternately into the main stream to form a periodic, square-wave pattern of exhaust composition. Air pulse injections increased O_2 concentration to 0.85% over a 0.5 s time span. CO pulse injections increased CO and H_2 to 1.2% CO and 0.4% H_2 over the next 0.5 s. The perturbation frequency was 1 Hz. The average gas composition for the honeycomb reactor was 0.75% CO, 0.25% H_2, 0.6% O_2, 16.3% CO_2, 10% H_2O, 1600 ppm NO, 280 ppm, C_3H_8, 280 ppm C_3H_6, and 40 ppm SO_2 with the balance nitrogen. Catalyst inlet and outlet gas compositions were determined using HC/CO/NO analyzers while raising temperature gradually from room temperature to 823 K to obtain HC/CO/NO conversions at different temperatures at a space velocity of 50,000 VHSV. The reaction temperature was measured by a thermal couple placed about 1 cm downstream of the monolithic catalyst.

Catalyst aging. Some catalysts were aged to simulate in-use catalyst operation before activity measurements. The laboratory honeycomb reactor aging was conducted in the simulated auto exhaust gas stream at 1173 K for 12 h. Some catalysts were aged in 10% steam air, and some aged in 10% steam–7% H_2 with the balance nitrogen, as specified later.

Catalyst characterization. Analytical electron microscopy (AEM), including bright field and annular dark-field imaging and X-ray emission spectroscopy, was used to characterize Pt and Rh particle size and composition of Pt–Rh catalysts after different pretreating and aging conditions. X-ray photoelectron spectroscopy (XPS) was used to monitor structural changes of Rh after different pretreatments. The AEM and XPS methods and procedures were reported in detail by Lakis *et al.* (16). Powder X-ray diffraction (XRD) data were collected for the catalysts on Philips APD 1700 diffracter operating at 45 kV and 40 mA. Temperature-programmed reduction (TPR) was done using 7% hydrogen in argon flow. Catalyst powders used for the AEM studies had compositions of 1.9 wt% Rh/Al_2O_3 and (0.65 wt% Pt–0.95 wt% Rh)/Al_2O_3.

RESULTS

Catalyst activity at 673 K. HC/CO/NO conversions were measured at 673 K to mimic catalyst performance during normal vehicle operating conditions. In order to simulate in-use catalyst performance, Pt and Rh catalysts were aged in the simulated auto exhaust stream at 1173 K for 12 h. HC/CO/NO conversions for the aged Pt/alumina, Rh/alumina, and Pt–Rh/alumina catalysts were obtained at 673 K in the simulated auto exhaust containing 40 ppm SO_2 at a space velocity of 50,000 VHSV. Results are summarized in Table 2. HC/CO/NO conversions are 80, 65, and 30% for the Pt/alumina; 22, 45, and 50% for the Rh/alumina; and 85, 75, and 67% on the Pt–Rh/alumina catalysts, respectively. It is clear that Pt-containing catalysts including Pt/alumina and Pt–Rh/alumina give higher HC/CO conversions, while Rh-containing Rh/alumina and Pt–Rh/alumina catalysts shows higher NO conversions. These results are in agreement with data reported in the literature, as summarized by Taylor, that in Pt–Rh three-way catalysts, Pt mainly

TABLE 2

HC/CO/NO Conversions for Pt and Rh Catalysts Aged in Simulated Exhaust at 1173 K

Catalyst	HC conversion (%)	CO conversion (%)	NO conversion (%)
Pt/alumina	80	65	30
Rh/alumina	22	45	50
Pt–Rh/alumina	85	75	67

FIG. 1. HC light-off curves for Pt and Rh catalysts aged in simulated exhaust at 1173 K.
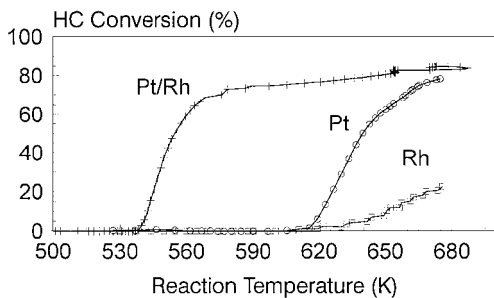

FIG. 3. NO light-off curves for Pt and Rh catalysts aged in simulated exhaust at 1173 K.

contribute to HC/CO oxidation and Rh is highly active for NO$_x$ reduction (1, 2).

HC light-off. Light-off performance was evaluated by measuring conversions at different temperatures while raising reaction temperature gradually from room temperature to about 773 K. HC light-off curves are shown in Fig. 1 for Pt and Rh catalysts aged in the simulated exhaust. For the Pt/alumina catalyst, HC conversion starts to increase at 623 K, and ~80% HC conversion is obtained at 673 K. On the Rh/alumina catalyst, HC conversion picks up at 623 K, and increases to ~22% at 673 K. This suggests that Pt catalysts are more active in HC conversion than Rh catalysts after aging. In contrast, HC conversion on the Pt–Rh/alumina catalyst starts around 540 K, and increases sharply to 70% around 560 K, and then gradually to 85% around 673 K. Note that at 560 K, the Pt/alumina and the Rh/alumina catalysts show zero HC conversion. Consequently, the high activity of the Pt–Rh/alumina catalyst suggests that there is a synergism between Pt and Rh in the Pt–Rh catalyst system.

CO light-off. Figure 2 shows CO light-off curves for the aged Pt and Rh catalysts. For the Pt/alumina catalyst, CO conversion starts around 610 K, and then increases to 65% around 673 K. On the Rh/alumina catalyst, CO conversion starts at temperature as low as 550 K, but increases slowly to 50% around 673 K. This suggests that Pt catalysts are more active for CO conversion than Rh catalysts at 673 K. By
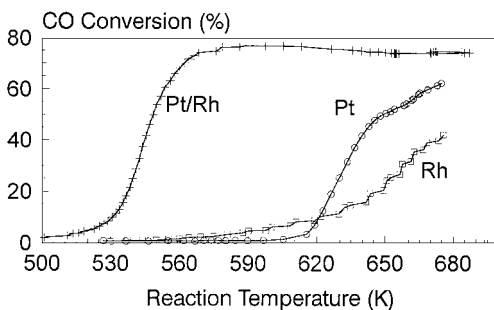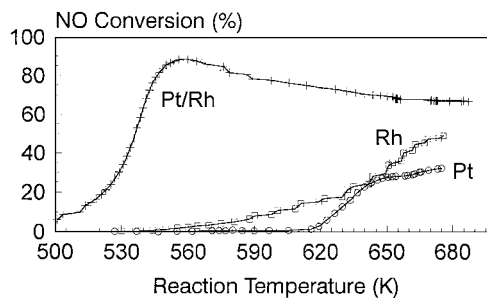
comparison, CO conversion on the Pt–Rh/alumina catalyst starts at 500 K and increases sharply around 540 K, to 75% around 560 K. At temperatures below 540 K, the Pt and the Rh catalysts show zero CO conversion. These results imply again that a synergism exists between Pt and Rh in the aged Pt–Rh catalyst system, as discussed above.

NO light-off. NO light-off curves for the aged Pt and Rh catalysts are summarized in Fig. 3. For the Pt/alumina catalyst, NO conversion starts around 620 K, and increases to 30% around 673 K. On the Rh/alumina catalyst, NO conversion starts around 550 K, and then increases slowly with increasing temperature, to 50% around 673 K. This result indicates that Rh catalysts are more active in converting NO than Pt catalysts. However, for the Pt–Rh/alumina catalyst, NO conversion starts at a temperature below 470 K, and increases to a maximum 88% around 550 K and then gradually decreases with increasing temperature to 67% around 673 K. It should be noted that at 550 K, the Pt–Rh/alumina catalyst showed the highest 88% NO conversion. This temperature is too low for NO reduction on either the Pt and the Rh catalysts to have any activities. Clearly, the aged Pt–Rh/alumina catalyst is much more active than individual Pt or Rh/alumina catalysts in converting NO, further supporting that a Pt/Rh synergism is responsible for the high activity observed on the aged Pt/Rh catalyst.

Light-off temperatures, defined here as the reaction temperature at which conversion reaches 50%, are summarized in Table 3 for the aged Pt and Rh catalysts. In general, the lower the light-off temperature, the higher is the catalyst activity. For HC/CO conversions, the light-off

FIG. 2. CO light-off curves for Pt and Rh catalysts aged in simulated exhaust at 1173 K.

TABLE 3

HC/CO/NO Light-Off Temperatures for Pt and Rh Catalysts Aged in Simulated Exhaust at 1173 K

Catalyst	T_{50}/HC (K)	T_{50}/CO (K)	T_{50}/NO (K)
Pt/alumina	640	655	NA
Rh/alumina	NA	673	670
Pt–Rh/alumina	560	560	540

TABLE 4

HC/CO/NO Light-Off Temperatures for Fresh Pt and Rh Catalysts

Catalyst	T_{50}/HC (K)	T_{50}/CO (K)	T_{50}/NO (K)
Pt/alumina	560	560	560
Rh/alumina	560	560	560
Pt–Rh/alumina	560	550	550

TABLE 5

HC/CO/NO Light-Off Temperature for Pt and Rh Catalysts Aged in Hydrogen at 1173 K

Catalyst	T_{50}/HC (K)	T_{50}/CO (K)	T_{50}/NO (K)
Pt/alumina	610	630	NA
Rh/alumina	570	560	560
Pt–Rh/alumina	—	—	—

temperature decreases in order of Rh > Pt ≫ Pt–Rh. For NO conversion, the light-off temperature decreases in order of Pt > Rh ≫ Pt–Rh. The Pt–Rh/alumina catalyst shows a light-off temperature ∼100 K lower than either the Pt/alumina or the Rh/alumina catalysts. It is therefore justified to use light-off temperature as an catalyst activity indicator. Testing of catalyst light-off performance suggests that Pt catalysts are more active for HC/CO conversions than Rh catalysts, and the reverse is true for NO conversion. However, the Pt–Rh catalyst is much more active in converting all three pollutants HC/CO/NO than individual Pt and Rh catalysts. The activity of the Pt–Rh catalyst is estimated one order of magnitude higher than the Pt or Rh catalysts assuming an activation energy of 25 kcal/mol. This superior activity of the aged Pt–Rh catalyst system is attributed to the synergism between Pt and Rh.

Fresh catalyst. In order to identify the origin of Pt/Rh synergism, light-off performance is characterized for fresh Pt and Rh catalysts, as shown in Table 4. All three catalysts, including Pt/alumina, Rh/alumina, and Pt–Rh/alumina, have nearly the same light-off temperatures for HC/CO/NO around 550–560 K. This is similar to the light-off temperature for the aged Pt–Rh/alumina catalyst. These results indicate that both fresh Pt and Rh catalysts are highly active in converting all three pollutants HC/CO/NO. There is no synergism between Pt and Rh observed in the fresh catalyst.

Catalyst aging in reducing condition. The simulated automotive exhaust composition perturbates around stoichiometry and mainly consists of rich cycles and lean cycles. In rich cycles, exhaust contains excess CO and HC which forms a net reducing environment. In lean cycles, exhaust contains excess oxygen forming a net oxidizing environment. Catalyst deterioration may take place in both rich and lean cycles. In order to simulate catalyst aging in rich cycles, catalyst aging in 7% hydrogen–10% steam with balance nitrogen at 1173 K was chosen. Table 5 summarizes catalyst light-off temperatures after the hydrogen aging. For the Rh catalyst, HC/CO/NO light-off temperatures are around 560 K, which are almost identical to that of the Pt–Rh catalyst aged in simulated exhaust. However, the Pt catalyst gives HC/CO light-off temperature of 610 and 630 K, respectively, and NO conversion never reaches 50% at tem-

perature below 773 K, the maximum temperature tested in this study. For the Pt–Rh catalyst, light-off temperature was not measured directly here; however, it is confirmed in an independent experiment that HC/CO/NO light-off temperatures are almost identical to that obtained on the Rh catalyst. Clearly, Pt catalysts are deactivated severely in the hydrogen aging; however, the Rh and Pt–Rh catalysts remain highly active for HC/CO/NO conversions. There is no Pt–Rh synergism observed in the Pt–Rh catalyst after hydrogen aging.

Catalyst aging in oxidizing condition. Catalyst aging in air at 1173 K was chosen to simulate catalyst deactivation in lean cycles. Light-off temperatures are summarized in Table 6. For the Pt catalyst, HC/CO light-off temperatures are 640 and 650 K, respectively, and NO conversion never reached 50% at temperature below 773 K. Comparing to the Pt catalyst performance after hydrogen aging, air aging results in higher light-off temperature, indicating a more severe deactivation. This is in agreement with data in the literature (17). For the Rh catalyst, HC/CO/NO light-off temperatures are 790, 800, and 700 K, respectively. In comparison with the Rh catalyst performance after hydrogen aging, it is clear that air aging results in severe loss of Rh catalyst activity. This again agrees with observations reported in the literature. However, the Pt–Rh catalyst shows HC/CO/NO light-off temperatures around 570 K after the air aging. This is almost same as that obtained in the Pt–Rh catalyst after aging in the simulated exhaust. Only the Pt–Rh catalyst remains highly active for converting all three pollutants HC/CO/NO after air aging. It is clear that a Pt–Rh synergism exists in the air-aged Pt–Rh catalyst.

TABLE 6

HC/CO/NO Light-Off Temperatures for Pt and Rh Catalysts Aged in Air at 1173 K

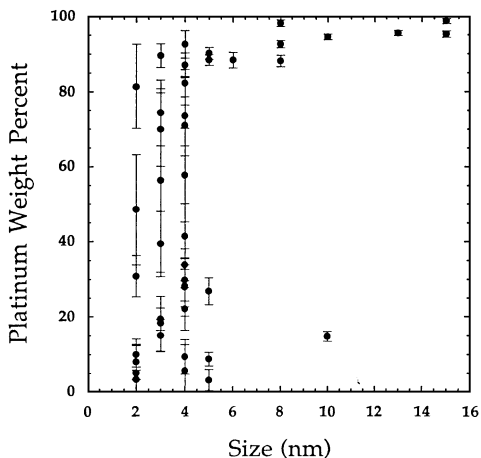| Catalyst	T_{50}/HC (K)	T_{50}/CO (K)	T_{50}/NO (K)
Pt/alumina	640	650	NA
Rh/alumina	NA	NA	700
Pt–Rh/alumina	570	560	550

FIG. 4. Particle size and composition of single metal particles in Pt–Rh/alumina catalyst aged in hydrogen at 1173 K.

AEM characterization. A mixture of 1.3 wt% Pt/Al$_2$O$_3$ catalyst and 1.9 wt% Rh/Al$_2$O$_3$ catalyst powders were milled to reduce particle size to 90% less than 10 μm, dried at 383 K for 12 h, and calcined at 773 K for 2 h to provide the catalyst powders for structural characterization. AEM was used to estimate particle size and composition of each individual metal particle. The method was reported in detail by Lakis *et al.* (16).

Pt/Rh aged in hydrogen. Figure 4 summarizes particle size and composition data of Pt and Rh metal particles collected on the Pt–Rh catalyst after aging in 7% H$_2$–10% steam with balance nitrogen flowing at 1173 K for 12 h. Particle size is shown on the X axis, and platinum concentration in weight percent of the metal particle is shown on the Y axis. Most particles have sizes between 2 to 4 nm. Some particles are as large as 15 nm. For small particles, Pt concentration varies from as low as 10% to as high as 90%. This result suggests that most particles contain both Pt and Rh and probably in the nature of Pt–Rh alloy. For the few large particles identified, Pt concentration is typically above 90%, indicating that the large metal particles are more close to Pt metal in nature. Summarizing all the metal particles identified, the average particle size is about 3 nm. Metal particle composition data are summarized in Fig. 5. Pt concentration, in weight percent, is shown on the X axis, and the number of metal particles containing Pt in the same percentile of concentration is shown on the Y axis. It is noted that most particles contain both Pt and Rh, indicating a Pt–Rh alloy formation during the hydrogen aging at 1173 K. For those large particles with a particle size above 8 μm, Pt is the dominant component. In this study, Pt and Rh have been placed separately on ~50-μm alumina granules by impregnation and then fixed on alumina support by calcination at 773 K. The Pt and Rh catalyst powders are then ball milled in deionized water medium to reduce average granule particle size to ~6 μm. It should be noted that

Pt and Rh concentration in the water medium was undetected after the milling process was completed, indicating that Pt and Rh did not migrate during the milling process. Therefore, the formation of Pt–Rh suggests that Pt or Rh nanometer-sized particles have migrated over micrometer distances and crossed the granule boundary to react with each other. Pt mobility is probably higher than the Rh as indicated by the fact that the large particles predominantly contain Pt.

Pt–Rh aged in air. AEM was used to examine the structure of the Pt–Rh catalyst aged in air at 1173 K for 12 h. Rh species are easily identified by the probe; however, no Rh-containing particles can be found in STEM images. In a separate experiment, XPS data confirm that Rh exists in Rh^{3+} exclusively in this catalyst. Pt occurs identified as 50-nm particles as seen in STEM images. XRD was used to characterize the structure, which confirms that Pt exists as 50-nm particles. No Rh-containing particles are detected by XRD. These results indicate that Rh exists in a highly dispersed form.

Pt–Rh catalyst aged in air followed by hydrogen aging. The Pt–Rh catalyst was first aged in steam air at 1173 K and then aged in 7% hydrogen and 10% steam with the balance nitrogen at 1173 K for 12 h. Rh particles were identified easily in STEM images, having a very uniform particle size distribution around 3 nm. Structure of Rh particles identified in STEM is also confirmed by particle composition analysis results as shown in Fig. 6. Rh concentration of metal particles is around 100%. All 3-nm particles contain Rh almost exclusively. Beside these 3-nm Rh particles, some 50-nm particles are identified which contain only Pt. It is clear that this catalyst contains essentially very small Rh particles and very large Pt particles. No Pt–Rh alloy is detected in this Pt/Rh catalyst after the hydrogen aging at 1173 K after the catalyst has been pretreated in air at 1173 K.

Rh catalyst aged in hydrogen. AEM was used to characterize the structure of the Rh catalyst after aging in hydrogen at 1173 K for 12 h. Rh is found to occur as 3-nm particles having a very uniform size distribution.
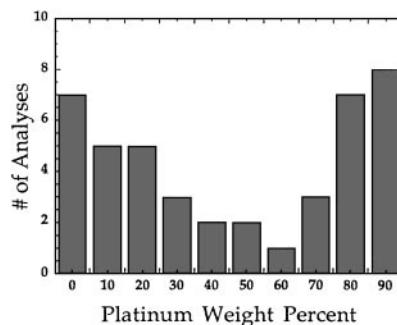

FIG. 5. Platinum concentration of single metal particles in Pt–Rh/alumina catalyst aged in hydrogen at 1173 K.
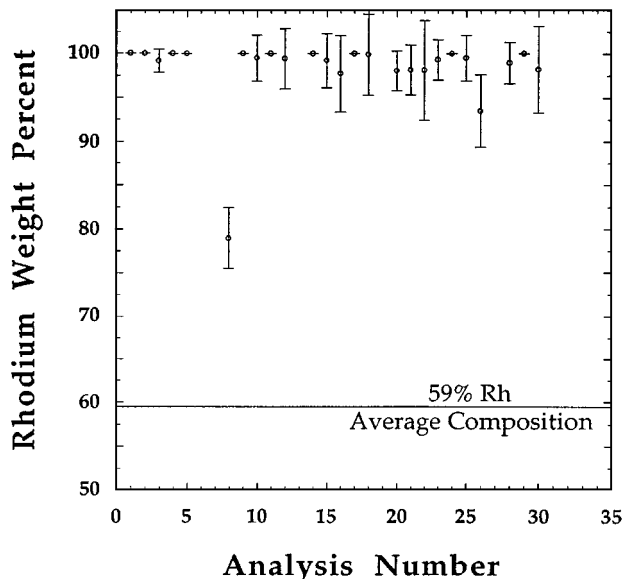
FIG. 6. Rhodium concentration of single metal particles in Pt–Rh/alumina catalyst aged in air followed by aging in hydrogen at 1173 K.

XPS characterization. Rh binding energy is determined using XPS to characterize catalyst structural changes after different treatments. For the Pt–Rh catalyst aged in air at 1173 K for 12 h, as shown in Curve A of Fig. 7, Rh exists as Rh^{3+} exclusively, as suggested by the sharp peak around binding energy of 311 eV. After subsequent treatment in

7% hydrogen–10% steam with balance nitrogen flowing at 773 K for 12 h, a small shoulder around 308 eV corresponding to Rh metal develops, while the peak around 311 eV remains being dominant, as shown in Curve B. After the hydrogen treatment at 973 K, as shown in Curve C, the intensity of the 308 eV peak increases significantly and the 311 eV peak decreases substantially. This result suggests more Rh is transformed from the oxide to the metal form. When the hydrogen treatment temperature is increased to 1173 K, the Rh peak around 308 eV becomes the dominant one, and the Rh^{3+} peak reduces to a small shoulder, as shown in Curve D. Clearly, a majority of Rh has been reduced to Rh metal in hydrogen treatment at 1173 K. The Rh^{3+} peak may be related to the rhodium oxide species formed during air exposure in the sample transportation process.

For the Rh catalyst aged in hydrogen at 1173 K, as shown in Curve F of Fig. 7, the Rh metal peak is the dominant one. A Rh^{3+} shoulder peak is also observed, attributed to Rh^{3+} formed during air exposure during sample transportation process. A temperature-programmed reduction experiment confirmed that for a Rh/alumina catalyst calcined at 773 K, a complete reduction of Rh oxide is achieved at temperatures below 873 K. For the Pt–Rh/alumina catalyst aged in hydrogen at 1173 K, as shown in Curve E of Fig. 7, a Rh metal peak is observed almost exclusively. From the microscopy experiments, all Rh has formed a Pt–Rh alloy during the hydrogen aging at 1173 K, as discussed above. No Rh^{3+} shoulder peak is observed even though this
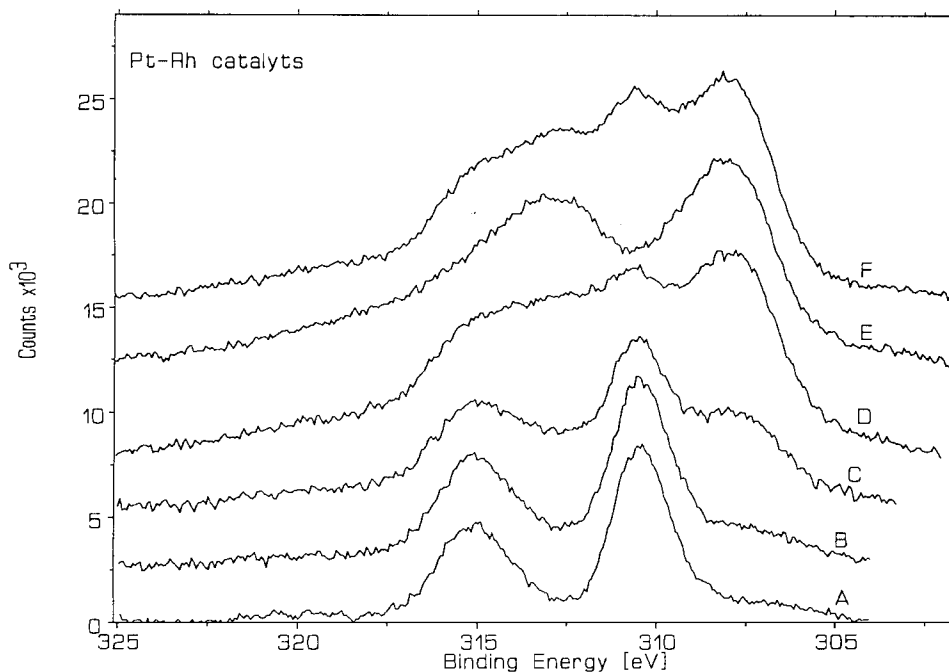

FIG. 7. Rh binding energy of Rh catalysts after various treatments. (A) 0.65 wt% Pt–0.95 wt% Rh/Al₂O₃ 1173 K/Air. (B) A + 773 K/hydrogen. (C) A + 973 K/hydrogen. (D) A + 1173 K/hydrogen. (E) 0.65 wt% Pt–0.95 wt% Rh/Al₂O₃ 1173 K/hydrogen. (F) 0.95 wt% Rh/Al₂O₃ 1173 K/hydrogen.

catalyst sample has been exposed to air during sample transportation, suggesting that the oxidation of Rh in the alloy is retarded by Pt.

DISCUSSION

Catalyst structural transformation. Pt and Rh particles supported on high surface area alumina are highly dispersed after calcination at temperature below 773 K. In this study, Pt and Rh were supported separately on different alumina granules. After the alumina granule size is reduced to 90% less than 10 μm, the average particle size is 5–6 μm distributed within a range of 1 to 10 μm. Catalyst structural changes observed with AEM, XRD, and XPS characterization are summarized in Fig. 8.

When the Pt catalyst is heated in hydrogen at high temperature, Pt particles finely dispersed in the fresh catalyst start to move and sinter, and some Pt agglomerates to 15 nm during hydrogen aging at 1173 K. If the Pt catalyst is heated in air, Pt particles agglomerate to much larger particles of ∼50 nm, after air aging at 1173 K. Such a low Pt dispersion was confirmed by hydrogen chemisorption in a separate experiment. This is in agreement with observations reported in the literature that Pt sinters much more severely under oxidizing conditions compared to reducing conditions (17). For the aging process in a simulated exhaust stream, Pt particles agglomerate in the reducing mode and sinter more severely in the oxidizing mode to form large Pt particles, i.e., about 50 nm, which are stable on the alumina support in the oxidizing condition at 1173 K. Once Pt agglomerates to 50-nm particles, then it will remain as such large particles in subsequent reducing cycles.

For the Rh/Al$_2$O$_3$ catalyst, Rh is highly dispersed as rhodium oxide particles on alumina after calcination at temperatures below 773 K. When this Rh catalyst is heated in hydrogen at a high temperature, Rh is reduced to metal and starts to migrate and sinter to 3-nm particles after hydrogen aging at 1173 K. It is impressive that Rh remains dispersed as relatively fine particles, having a dispersion around 30% even after the 1173 K aging. The Rh dispersion estimated by STEM is in agreement with chemisorption measurement results. It is clear that Rh particles are much smaller than the Pt particles after 1173 K hydrogen aging, suggesting that Pt has a mobility much higher than Rh under reducing conditions. If the Rh catalyst is heated in air at high temperature, rhodium oxide particles start to react with the gamma alumina support, forming a highly dispersed Rh–Al–oxide species nondetectable by STEM and XRD, which is much more difficult to reduce in hydrogen compared to the rhodium oxide particles supported on alumina. Reduction temperature increases from 500 K to about 900 K, as measured by TPR. This supports observations reported in the literature that Rh diffuses into the bulk of alumina support to form nonactive Rh–aluminate species (9, 10, 18). For the Pt–Rh catalyst aged in simulated exhaust, Rh should be reduced to form 3-nm Rh particles in the reducing mode and then be oxidized and subsequently react with the alumina support to form the Rh–aluminate species in the oxidizing mode. The final structure of Rh in the catalyst aged in simulated exhaust is probably a mixture of 3-nm Rh particles and Rh–aluminate species. The ratio may depend largely on aging exhaust gas composition and the finishing process.

The Pt–Rh catalyst prepared here consists of a physical mixture of Pt/Al$_2$O$_3$ and Rh/Al$_2$O$_3$ particles, with the alumina supporting Pt and Rh being smaller than 10 μm. When the fresh Pt–Rh catalyst is heated in hydrogen at high temperature, Pt starts to move and probably migrate across the boundary between two alumina granules and react with Rh metal to form a Pt–Rh alloy. Rh has a much lower mobility and, therefore, probably contributes little to the across-boundary migration responsible for the Pt–Rh alloy formation.

When the fresh Pt–Rh catalyst is heated in air at high temperature, Pt particles start to agglomerate and form 50-nm Pt particles after 1173 K, and Rh reacts with alumina support to form a Rh–aluminate species. Following the air aging at 1173 K, when the Pt–Rh catalyst is heated in hydrogen at 1173 K, Rh is reduced and forms 3-nm Rh metal particles. However, Pt particles do not experience further structural change since Pt has agglomerated to very stable 50-nm Pt particles in the preceding air aging at 1173 K. The lack of Pt–Rh alloy formation suggests that Rh does not migrate over long distances in order to react with the small number of large Pt particles.

For the catalyst aged in simulated exhaust, Pt and Rh may react with each other initially to form Pt–Rh alloy in the reducing mode. Ultimately, Pt should agglomerate to 50-nm Pt particles stable in the oxidizing mode. The initial Pt–Rh alloy formed in the reducing mode should be oxidized, and then Pt agglomerates to 50-nm particles, and
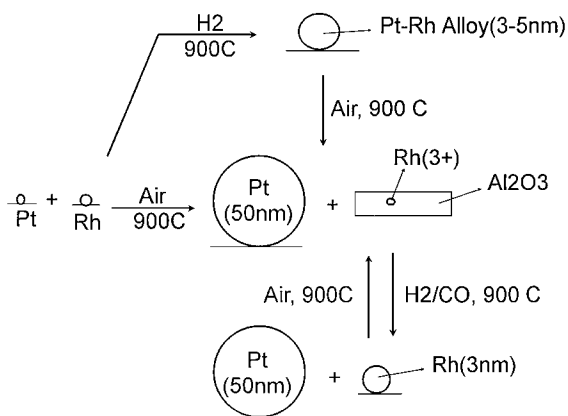

FIG. 8. Structural transformation of Pt–Rh catalyst in different treatments.

Rh reacts with the alumina support to form Rh–aluminate species in the oxidizing mode. Rh may react with alumina to form Rh–alumina species in the oxidizing mode and then reduced to form 3-nm Rh metal particle in the subsequent reducing mode. The ratio is determined by the exhaust gas composition and the aging finishing process.

Structure–performance correlation. Finely dispersed Pt particles are highly active for three-way conversion of HC/CO/NO. However, at high temperature, Pt particles agglomerate in a reducing environment and sinter more severely in an oxidizing environment. The sintered Pt catalyst has a significantly lower activity and largely loses its ability to reduce NO to nitrogen. Finely dispersed Rh particles are highly active for the HC/CO/NO three-way conversion. At a high temperature of 1173 K, Rh remains as finely dispersed 3-nm Rh particles under the reducing condition and have high three-way catalyst activity even after high-temperature aging in hydrogen. However, Rh reacts with the alumina support at 1173 K in air to form an inert Rh–aluminate species for TWC reactions. Such inert Rh–aluminate species are very stable; no significant reduction and regeneration to Rh metal particles are observed in simulated exhaust or in 7% hydrogen–10% steam at 773 K. Rh/Al_2O_3 catalysts deactivate severely after high temperature air aging.

Fresh Pt/Rh catalysts, i.e., a mixture of finely dispersed Pt and Rh catalyst powders, are highly active for TWC conversion, as predicted based on activities of fresh Pt and Rh catalysts. Heating the Pt and Rh catalyst mixture in hydrogen at high temperature results in the formation of finely dispersed Pt–Rh alloy particles, which are highly active TWC catalysts. The activities of the Pt–Rh alloy particles in the Pt/Rh catalyst and the Rh metal particles in the Rh catalyst after 1173 K hydrogen aging are almost identical, indicating that Pt–Rh alloy formation does not improve or reduce catalyst activity significantly. Aging Pt–Rh catalysts in simulated exhaust should result in a catalyst structure of 50-nm Pt particles, 3-nm Rh particles, and the Rh–aluminate species. Only the 3-nm Rh particles are highly active for TWC reactions. After air aging at 1173 K, the Pt–Rh catalyst should contain only 50-nm Pt particles and the Rh–aluminate species, both of which have low activities for TWC reactions. However, the air-aged Pt–Rh catalyst is highly active for TWC reactions, as demonstrated experimentally. This leads to a model that in the Pt–Rh catalyst, Pt facilitates regeneration of the inert Rh–aluminate species to active Rh metal particles in the exhaust cycling between net oxidizing and reducing compositions, probably through hydrogen spillover mechanism, as shown in Fig. 9. In order to support this model, the 1173 K air-aged Pt, Rh, and Pt–Rh catalysts were reduced in 7% hydrogen and 10% water with nitrogen balance flowing at 773 K for 12 h, the Pt/alumina and the Rh/alumina catalysts remain as a low-activity TWC catalyst, and the Pt–Rh catalyst gives high TWC activity. The
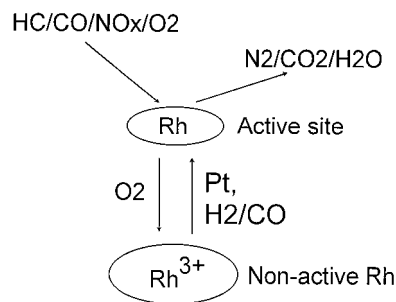

FIG. 9. Reaction paths of HC/CO/NO conversions for in-use Pt–Rh catalysts.

1173 K oxidized Rh catalyst showed a higher TWC activity after the 773 K hydrogen treatment and an almost fully restored activity after hydrogen treatment at 1173 K, supporting that Rh reduction to metal particles is the mechanism responsible for the catalyst regeneration. It is also found that the air-aged Pt–Rh catalyst can be regenerated in simulated exhaust replacing the CO/H_2 mixture with equivalent pure CO or pure H_2. This result suggests that both carbon monoxide and hydrogen are effective at facilitating regeneration of the inert Rh–aluminate species in the exhaust stream under normal operating conditions. A NO light-off temperature of 560 K has been obtained on the Pt–Rh catalyst aged in air at 1173 K, indicating that H_2 spillover has taken place and leads to regeneration of the inert Rh–aluminate species to Rh metal particles at temperature around 560 K.

CONCLUSION

Highly dispersed Pt and Rh are active catalysts for three-way conversion of HC/CO/NO. However, Rh is readily deactivated by forming an inert Rh–aluminate species under oxidizing condition at high temperature. Pt agglomerates to large Pt particles and loses its activity after high-temperature exposure. For in-use Pt–Rh catalysts, Rh is the main active component responsible for TWC conversions. The main function of Pt is to keep the Rh active as Rh metal particles. This is achieved probably through a mechanism of H_2 spillover on Pt particles which facilitates the regeneration of inert Rh–aluminate species formed under oxidizing conditions at high temperatures.

REFERENCES

1. Taylor, K. C., *in* "Catalysis: Science and Technology" (J. R. Anderson and M. Boudart, Eds.), Vol. 5. Springer-Verlag, Berlin, 1984.
2. Taylor, K. C., *Catal. Rev.-Sci. Eng.* **35**(4), 457 (1993).
3. Taylor, K. C., "The Catalytic Chemistry of Nitrogen Oxides" (R. Klimisch and J. G. Latson, Eds.), Plenum, New York, 1975.
4. Gandhi, H. J., Piken, A. G., Shelef, M., and Delosh, R. G., Paper No. 760201, Presented to Society of Automotive Engineers, 1976.

5. Mooney, J. J., Thompson, C. E., and Dettling, J. C., Paper No. 770365, Presented to Society of Automotive Engineers, 1977.

6. Taylor, K. C., *Ind. Eng. Prod. Res. Dev.* **15**, 264 (1976).

7. Schlater, J. C., Taylor, K. C., and Sinkevitch, R. M., Paper presented at the Advances in Catalytic Chemistry Symposium, Snowbird, Utah, 1979.

8. Kim, Y., Shi, S. K., and White, J. M., *J. Catal.* **61**, 374 (1980).

9. Yao, H. C., Japar, S., and Shelef, M., *J. Catal.* **50**, 407 (1977).

10. Yao, H. C., and Gandhi, H. S., *J. Catal.* **61**, 547 (1980).

11. Ohara, T., *in* "The Catalytic Chemistry of Nitrogen Oxides" (R. Klimisch and J. G. Latson, Eds.), Plenum, New York, 1975.

12. Cooper, B. J., Harrison, B., Shutt, E., and Lichtchenstein, L., Paper No. 770367, Presented to Society of Automotive Engineers, 1977.

13. Van den Bosch-Driebergen, A. G., *et al.*, *Catal. Lett.* **2**, 73 (1989).

14. Oh, S. H., and Carpenter, J. E., *J. Catal.* **98**, 178 (1986).

15. Hu, Z., *J. Chem. Soc. Chem. Commun.* 879 (1996).

16. Lakis, R. E., Lyman, C. E., and Stenger, H. G., Jr., *J. Catal.* **154**, 261 (1995).

17. Yao, H. C., Sieg, M., and Plummer, H. K., *J. Catal.* **59**, 365 (1979).

18. Wan, C. Z., and Dettling, J. C., "Catalysis and Automotive Pollution Control" (A. Crucq and A. Frennet, Eds.), Elsevier, Amsterdam, 1987.